S PIN
P HYSICS
I NTER-
N ATIONAL

Integrated Proposal on First Round Experiments With the Polarized Beam Facility

R. Ditzler, D. Hill, H. Spinka, R. Stanek, K. Toshioka
D. Underwood and A. Yokosawa

Argonne National Laboratory, Argonne, Illinois

K. Imai, R. Kikuchi, K. Miyake, T. Nakamura, K. Nishimura,
N. Sasao and N. Tamura

Kyoto University, Kyoto, Japan

H. Azaïez, K. Kuroda, A. Michalowicz, D. Perret-Gallix

LAPP, Annecy, France

G. Shapiro

Lawrence Berkeley Laboratory
University of California, Berkeley, California

N. Amos, M. Block, C. LeRoy, D. H. Miller and S. Zucchelli

Northwestern University, Evanston, Illinois

M. Corcoran, H. E. Miettinen, G. S. Mutchler,
G. C. Phillips and J. B. Roberts

Rice University, Houston, Texas

J. Bystricky, F. Lehar, A. DeLesquen, J. Movchet and L. Van Rossum

Saclay, France

V. Apokin, A. Derevschikov, Y. Matulenko, A. Meschanin, S. Nurushev,
V. Solovyanov and A. Vasilyev

Serpukhov, USSR

R. Birsa, F. Bradamante, S. Dalla Torre-Colautti, M. Giorgi, L. Lanceri,
A. Martin, P. Moras, A. Penzo, P. Schiavon and A. Villari

INFN, Sezione di Trieste, Trieste, Italy

Scientific Spokesman:
A. Yokosawa
Argonne National Laboratory
Telephone (312) 972-6311

September 8, 1981

Abstract

This document constitutes a proposal to perform simultaneously substantial parts of experiments described in proposals previously submitted (June, 1981).

P676 (Scientific Spokesman, Shapiro)

"An experiment to measure $\Delta\sigma_L^{Tot}$ in p-p and $\bar{p}$-p scattering between 100 and 500 GeV/c."

P-678 (Kuroda)

"Proposal to study the spin dependence in inclusive π° and direct gamma production at high $p_\perp$ with the polarized proton beam facility at Fermilab."

P674 (Roberts)

"Asymmetries in inclusive pion and kaon production at large-x with a polarized beam."

P-677 (Penzo)

"A study of the spin dependence in the inclusive production of lambda particles with the polarized beam at Fermilab."

Table of Contents

Page

I. Introduction and Summary..... 4

II. Physics Goals of this Proposal..... 6

III. Data Acquisition..... 9

IV. Details of Proposed Experiments.....12

A. Helicity Asymmetry in pp and $\bar{p}p$ Total Cross Sections.....12

B. Neutral-Pion Asymmetry Measurement.....16

C. High-x Charged Meson Production.....20

D. Large-x Λ°, K° Production.....23

V. Equipment Needed.....26

References.....27

Figure Captions.....28

I. Introduction and Summary

In this paper, we are proposing a single experimental setup to accomplish simultaneously substantial parts of the objectives detailed in the previously submitted proposals P-676, 678, 674, and 677. We have used the following criteria to select portions of our complete program for the first-round experiments:

i) Exploit fully every possibility for simultaneous use of beam time,

ii) Minimize the complexity of the data-taking mode,

iii) Economize on the apparatus.

According to these criteria we have singled out a group of measurements which should be prepared with high priority in order to ensure a variety of early results from the polarized beam facility. As suggested by the PAC in June, 1981 we describe an initial set of experiments in the context of 200-GeV/c operation, but our proposed setup is in general compatible with 400 or 500 GeV running.

We have a design for a 200-GeV/c conventional-magnet beam line. (A more detailed report is being prepared jointly by Fermilab and Argonne.) This beam differs from the full-energy beam line in the following respects:

a) No superconducting elements are used in the beam.

b) Only eight conventional quads are needed.

c) Beam intensities (plus and minus polarizations simultaneously) are about $2 \cdot 10^7$/spill by tagging of particles. The TEVATRON spill allows tagging of $3 \cdot 10^7$ particles. Shorter spills would require corresponding reduction of the number of particles/spill.

d) More dipoles are needed; 18 instead of 16.*

---

* For discussion of "why are the number of dipoles and power requirements not significantly reduced?", see a joint Fermilab - Argonne report (in preparation) discussed earlier.

e) Power consumption is 1.6 MW instead of 2.0 MW.*

f) Beam-line acceptance is reduced to 2/3 of the original design.

g) The beamline could be brought into operation early in the Tevatron program with performance adequate for some parts of the physics program and with minimal capital costs.

Figure 1 shows the experimental setup for the measurement of helicity asymmetry for the total cross section, the A_N measurements of π° production, $\pi^\pm$ production, and $\Lambda^\circ(K^\circ)$ production measurements.

We will allocate the first 1200 hours of beam time at 200 GeV/c as follows:

i) First 300 hours for $\Delta\sigma_L^{Tot}(pp)$ including tuning.

ii) 300 hours for $\Delta\sigma_L$ $(\bar{p}p)$.

iii) 600 hours for simultaneous measurements using a hydrogen target for A_N in large-$p_\perp$ π°, large-x $\pi^\pm$, and Lambda production.

We expect to make measurements with statistical precision as indicated in section V-A (pg. 15), Tables I, II, and III (pgs. 20, 22, and 25 respectively).

While $\Delta\sigma_L$ data taking is in progress, we plan to tune the detectors for A_N measurements, and we will attempt to measure A_{LL} in π° production.

II. Physics Goals of this Proposal

There are already several experimental indications that spin effects are significant at high energy:

-- Measurements of inclusive pion production in proton-proton collisions have revealed sizeable asymmetries at 6 and 12 GeV/c for $\pi^{\pm}$ [1], and at 24 GeV/c for π° ($\simeq$ - 20% at $p_{\perp} \simeq 2$ GeV/c)[2].

— Spin-correlation parameters, at the highest energies at which they have been measured (12 GeV/c), are seen to have large values,[3] and

-- Hyperons produced inclusively off nuclei and hydrogen are observed to have high polarizations,[4]

The presence of these large effects, particularly in inclusive reactions, was unexpected because of the complexity of events and it was considered unlikely that contributions from different channels would add in such a way as to produce a large effect.

The observation of substantial effects suggests that the underlying processes involved might be simple at the level of constituents.

Also a recent SLAC experiment[5] measuring inelastic scattering of longitudinally polarized electrons on longitudinally polarized protons reports a large asymmetry, implying that proton helicity orientation is communicated to the constituent quarks. Thus spin dependence in quark-quark collisions can be inferred from measurements of spin dependence in proton-proton collisions in appropriate kinematic regions.

With the advent of the Fermilab polarized beam we will have a unique facility to investigate these processes systematically.

In the first-round experimental program proposed we intend to start by exploring the spin dependence of the interactions in a global way by a straightforward experiment measuring the total cross-section difference in pp and $\bar{p}p$ between the states with helicities of target and beam parallel and antiparallel.

$$\Delta\sigma_L^{Tot} = \sigma^{Tot}_{(\overrightarrow{+})} - \sigma^{Tot}_{(\overrightarrow{+})} .$$

Helicity asymmetries in total pp cross section were found to be unexpectedly large at low energies[6] and we are led to expect that they may persist into the region of Fermilab energies. Straightforward extrapolation for the present data suggests $\Delta\sigma_L \simeq -6/p_{lab}$ in mb units. However, the unpolarized total cross-section in pp scattering rises by a few millibarns in the Fermilab energy range, and we are interested in the extent to which parallel and antiparallel initial helicities participate in this rise.

In $\bar{p}p$ interactions there are also good reasons to expect polarization effects at the highest energies. In any process at relativistic energy involving the annihilation of spin $-\frac{1}{2}$ particles into vector intermediate states, a reaction with initial particles having like helicities is almost completely supressed (by a factor γ) relative to the rate for the same reaction in a state of opposite helicities.

Measurements of $\Delta\sigma_L$ can be immediately followed by measurements of single-spin asymmetries in inclusive reactions:

$$A_N = \frac{E\frac{d^3\sigma}{dp^3}\uparrow - E\frac{d^3\sigma}{dp^3}\downarrow}{E\frac{d^3\sigma}{dp^3}\uparrow + E\frac{d^3\sigma}{dp^3}}$$

(the arrows refer to the transversity of the incoming proton).

Studies of the inclusive production of neutral pions around $x \approx 0$ and large $p_\perp$, of charged pions at large x, and of $\Lambda^\circ(K^\circ)$ at large x will be carried out simultaneously. With these measurements we directly address the puzzling questions raised by the previously quoted experimental results:

- How is the spin in a transversely polarized proton transmitted to constituents, and how does this spin affect inclusive yields as a function of x_F and of $p_\perp$?
- If pairs of quarks produced in the strong interaction are polarized (as seems to be indicated by the polarization in hyperon production) what is their origin and the polarizing mechanism?
- If the large asymmetry observed in π° production persists at large $p_\perp$(~ 4-5 GeV/c) and large energy (200 GeV/c) what might be the implications for perturbative QCD of hard scattering (which predicts vanishing single-spin effects)?

We expect that our first round of relatively simple experiments in the polarized proton beam will yield significant results relevant to the above questions.

III. Data Acquisition

General Requirements: We will need the facility to acquire data from all four experiments simultaneously. (Three will run simultaneously and will be tuning during $\Delta\sigma_L$.)

Dead time from either of the two high trigger-rate experiments (Λ° and large-x $\pi^\pm$) should not interfere with other experiments. Program modifications, hardware modifications, or hardware failures in any one experiment should not affect the others significantly. Data on tape from each experiment should be readily accessible without conflict with other experiments at least during early stages of running. Data tapes from each trigger may be sent to different home institutions for final analysis.

We describe one way to meet all these requirements without duplication of a significant number of proportional chambers. The basis is the use of two latches for each chamber (for Λ° and $\pi^\pm$) and perhaps three for upstream chambers (for π°, Λ°, and $\pi^\pm$). With separate data latching, one experiment does not introduce dead time or interact with another experiment. We are investigating the relative costs of various ways to provide this kind of performance. Trigger hodoscopes and fast MWPC outputs required for more than one experiment can be fanned out. Separate triggers of various levels would be used for each experiment. At least two data acquisition computers using Camac would be used.

We are considering using two computers "A" and "B" such as PDP 11-45's or possibly smaller, each assigned to a high data-acquisition rate experiment ($\pi^\pm$ or Λ°). The low-acquisition-rate data for such items as scalers in the $\Delta\sigma_L$ experiment and target polarization will be recorded in either of the two computers. The use of parallel data systems all the way from MWPC to tape

drive would allow tuneup of three rather complex experiments without interference and also eliminate dead-time problems. A larger computer, perhaps one of the acquisition computers, could be used for extensive histograming for tuning and monitoring. With present resources, we could have two PDP 11-45 type computers available which might be adequate. A system with several small computers tied to one larger one has advantages in terms of tuning up several experiments. It appears that ample time is available to study these options.

Data Handling Schemes

Function	Trigger/Process	Camac	Output
Beam Momentum Selection	Matrix (Hodoscope)	Matrix Tags/Event	To tapes "A" and "B"
Beam Polarization Selection and Beam Intensity	Matrix (Pol - Mom)	Matrix Tags/Event, Polarization Magnitude and Sign/Event, and Matrix Scalers/Spill	To tapes "A" and "B"
Beam Polarimeter	Matrix (Hodoscope) Fast ADC (Hodoscope)	Scalers/Spill	To tapes "A" and "B"
Target Polarization	Hardware Processor	Special/Spill	To tapes "A" and "B"
$\Delta\sigma_L$(pp or $\bar{p}p$)	Matrix (Hard-Wired Processor)	Matrix Scalers/Spill	Tape "A" or "B"
$A_N(\pi^\circ$ Inclusive)	Lead Glass → Fast ADC → Fast Arithmetic → Fast Microprocessor	Processor Output (Including ADC, $p_\perp$, Mass), MWPC, and Hodo-Tags/Event	Tape "A" or "B"
A_N ($\pi^\pm$ Large x)	Standard Nim or Matrix	MWPC, Hodo-Tags, and C ADC	Tape "A"
$A_N(\Lambda^\circ)$, $D_{NN}(\Lambda^\circ)$	Fast Pretrig → Fast Processor	MWPC, Hodo-Tags, and C ADC	Tape "B"

Note: "A" and "B" refer to two separate computer systems.

A. Expected Trigger Rates

Experiment	Expected Good Events/Spill	Hardware Limit 10-sec Spill	Maximum Expected Computer Interrupt Rate
π°	~ 250	~ 5 K	~ 500/10 sec
Λ°	~ 1.5 K	~ 10 K	~ 3 K/10 sec
$\pi^\pm$	~ 1.5 K	~ 10 K	~ 3 K/10 sec
$\Delta\sigma_L$	2×10^7 max	2×10^8	

B. Words Transferred Per Computer Interrupt

Experiment	MWPC 16-bit Words	ADC Words	Scaler 16-Bit Words	Hodo-Tag Words
π°	~ 100	744 (may be reduced)	80	10
Λ°	~ 150	>4	> 80	10
$\pi^\pm$	~ 150	>4	80	10
$\Delta\sigma_L$	0	0	> 200	0

C. Data Transfer Rates

Experiment	Max. Expected Data Transfer Rate (16-Bit word/sec)	Remark
π°	50 K (may be reduced)	We expect that
Λ°	75 K	our computer system
$\pi^\pm$	75 K	will transfer data at
$\Delta\sigma_L$	Data transferred after each spill	250 K words/sec.

IV. Details of Proposed Experiments

Much of the description of detectors shown in Fig. 1 is contained in the original proposals. The new layout optimizes compatibility and possibilities of simultaneous running.

The beam is described in Fermilab proposal E-581 and the 200-GeV/c beam will be described in a separate note jointly prepared by Fermilab and Argonne personnel.

In addition, there are detectors in the polarized beam which are common to all experiments. We plan to use a number of finely grained hodoscopes ($\sigma \simeq$ 1-2 mm) placed in various positions along the beam line to i) tag both the polarization and momentum of beam particles by recording their transverse (x and y) positions in the intermediate focus region and ii) determine the direction and the transverse position at the experimental target for the incident particles HB1, HB2.

A "snake system"* consisting of eight dipole magnets will allow the correlation between polarization and phase space to be flipped frequently and minimize the systematic errors.

A. Helicity Asymmetry in Total pp and $\bar{p}p$ Cross Sections

This experiment will be a standard transmission experiment with the detectors specially designed for a high-divergence beam.

The longitudinally polarized beam passes through the scintillator hodoscopes (HB_1 and HB_2,) and interacts with the polarized proton target. The unscattered beam and forward-scattered particles pass through scintillator

---

* For details, see E-581 (revised) dated May 1, 1981.

hodoscopes (HB_3 to HB_6). Veto counters, Cerenkov counters, and analyzing magnets help reject inelastic events, and reactions in which mesons appear.

The hodoscopes in this experiment are expected to be used for the polarimeter[7] which measures tranverse beam polarization through elastic scattering in the Coulomb-interference region. With a longitudinally polarized beam, the polarimeter cannot monitor the beam polarization directly during the actual experiment, and there is no conflict in using the same apparatus for both purposes. Beam polarization will be checked periodically by changing to transverse spin and inserting H_2 target or depolarizing the polarized target.

We will use a standard, longitudinally polarized proton target, in a superconducting solenoid magnet. A target material such as ethylene glycol or propanediol, 10% hydrogen by weight and with a free proton density of .07 gm/cm^3, can be used to reliably obtain polarizations above 80%. More exotic materials, such as solid NH_3, have been investigated because of their higher fractional hydrogen content, and may be used if the state of the art warrants it at run time.

Matrix logic will be used to reject multi-particle events, and other obviously inelastic or large-angle scattering events. For tracks that are nearly collinear, before and after the target, a hard-wired calculation of the scattering angle θ will be executed, and a corresponding scaler incremented. Additional scalers will record the number of incident tracks and other pertinent matrix outputs. All scalers will be read into an on-line computer after each spill. In addition, magnet currents, target polarization, and hodoscope hit-patterns will be sampled periodically to monitor the data.

Beam passing through the polarized-proton target is attenuated by both the free polarized protons and the rest of the material. The number of particles, N_i (corrected for efficiency), transmitted through the target into the ith element of solid angle covered by segments of the transmission hodoscope is given by:

$$N_i^{\pm} = N_0^{\pm} \exp\left[-\alpha_i - \frac{1}{A}\left(\sigma_i \pm P_B P_T \frac{\Delta\sigma_{L,i}}{2}\right)\right], \qquad (1)$$

where ± refers to antiparallel (+) or parallel (-) beam and target polarizations, N_o is the number of incident beam particles, α_i is the attenuation constant for everything in the target except free hydrogen, σ_i is the integrated differential cross section from the ith solid angle subtended, $A = (N_A \rho_F L)^{-1} = 2320$ mb is the target constant for free hydrogen, N_A is Avogadro's number, $\rho_F = 0.0714$ g/cm^3 is the free-proton density, $L = 10$ cm is the target length, and $P_B = 0.45$ and $P_T = 0.8$ are the magnitude of the beam and target polarization, respectively.

The partial cross-section difference for each counter, $\Delta\sigma_{L,i}$, is calculated from these numbers by:

$$\tanh \frac{\Delta\sigma_{L,i} P_B P_T}{2A} = -\frac{N_i^+/N_0^+ - N_i^-/N_0^-}{N_i^+/N_0^+ + N_i^-/N_0^-} \quad . \qquad (2)$$

RATES AND RUN PLAN:

The statistical accuracy of the $\Delta\sigma_L$ measurment is expressed by:

$$\Delta(\Delta\sigma_L) = \frac{2A}{P_B P_T} \left(\frac{1-T}{T}\right)^{1/2} \frac{1}{\sqrt{N_o}} \ ,$$

where T is the fraction of the beam transmitted by the entire target and A is the target constant for free hydrogen. For this target T is about .85. We have A = 2320 mb for a 10-cm ethylene glycol with P_B = 0.45 beam polarization and P_T = 0.8 target polarization.

$$\Delta(\Delta\sigma_L) = 4800 \text{ mb}/\sqrt{N_o}$$

Our experience shows that we can easily achieve an accuracy of ± 100 microbarns with techniques used in previous experiments.[8] Note that the dominant contributions to the attenuation from the unclear part of the polarized target exactly cancel. The efficiencies also cancel to first order because the beam polarization is flipped on alternate pulses.

With proper care it is reasonable to aim for an accuracy of ± 10 microbarns. This level of precision will be necessary especially if the measured values turns out to be small. This level of precision requires 2×10^{11} incident protons. With 10^7 incident protons, of each sign of polarization, per spill every 50 seconds, this translates into 150 hours of data-taking. We also need 150 for tune-up and for checking the geometry to reduce systematic errors.

For the anti-proton beam, with its lower intensity, we cannot achieve the same level of statistical accuracy. We ask for 300 hours of beam time, which will include both checking-out and data-taking. With an intensity of 10^6 antiprotons per spill, the achievable statistical accuracy is ± 25 μb.

The apparatus for inclusive measurements can be checked out while the pp and $\bar{p}p$ data are being collected.

B. Neutral-Pion Asymmetry Measurement

Photons from the decay of π^0's produced by the interaction of protons on either a LH_2 or polarized target are detected in the two Pb-glass spectrometers G_1 and G_2. At p_{in} = 200 GeV/c the spectrometers are placed 10 m downstream of the target and centered around θ = 97 mrad which corresponds to x_F = 0. The azimuthal angle subtended by each spectrometer is ± 22.5° with respect to the horizontal plane.

The scintillation hodoscopes V_1 and V_2 immediately in front of the Pb-glass spectrometers, are constructed in three planes for segmentation in the X, Y, and U directions; these have spatial resolutions of 4 cm and serve to localize charged particles which accompany γ's.

The acceptance of the detector in x_F-$p_\perp$ space in shown in Fig. 2 for p_{in} = 200 GeV/c.

The two-gamma spectrometers comprise a major part of the detector. Each consists of 372 Pb-glass cells (3.8 x 3 x 45 cm) stacked to form a trapezoidal array as shown in Fig. 3. The Cerenkov light is collected by a photomultiplier at the rear of each cell. The detector elements and the design of the associated electronic system will be similar to those developed by the IHEP-IFSN-LAPP Collaboration for the GAMS 4000 spectrometer at CERN. This detector has shown remarkable spatial resolution (± 1 mm at 200 GeV), resulting from an optimal choice of tranverse dimensions of the Pb-glass cells.

To accommodate high event rates the integrated charge in each cell is digitized with its own ADC. Pedestal subtraction and energy normalization are performed automatically by a fast processor. Relative gains (PM + ADC) will be monitored under microprocessor control with an LED system between spills to

achieve a long-term stability better than 1%. The energy resolution has been measured for a spectrometer of this type; at full width half-maximum (FWHM) it is

$$\Delta E/E = 0.025 + 0.13/\sqrt{E}\ (\text{GeV})$$

giving ± 2.5% at 25 GeV. Linearity has been studied with electrons from 40 GeV, and no deviation larger than 1% was observed.

Energies and coordinates (using the method of moments) will be evalutated on-line. This provides the possibility for on-line calculation of gamma-gamma invariant mass and kinematics, and allows one to impose event selection criteria if necessary before recording data on tape. With reasonable estimates for processing times we conclude that as many as 500 events/sec can be recorded even with large multiplicities.

Fast discriminators sample the integrated charge in each cell. Thresholds are adjusted so that the detector is triggered when an energy greater than 10 GeV is deposited in any cell. This allows efficient detection of π°'s emitted near $x_F \approx 0$ and $p_\perp > 2.0$ GeV/c. If rates are too high the discriminator thresholds can be increased or the hodoscopes V_1 and V_2 can be used to reject clusters associated with charged particles. It is apparent, however, that event rejection is preferably executed off-line after careful study so that no bias is introduced in the inclusive final states.

To obtain a 'clean' sample of π° events all data must be subjected to extensive off-line analysis. Backgrounds due to improperly paired γ's will be estimated using Monte Carlo simulation with reconstructed π°'s as input. Contamination of the final sample by π°'s from decay of inclusively produced

η°'s, ω°'s, and K_s°'s can be reasonably estimated from available measurements and models which relate charged and neutral production. This contamination will be small at high $p_\perp$.

RATE AND ERROR ESTIMATES:

Rates for π° production have been estimatd with the following assumptions:

P_{in} = 200 GeV/c

Beam Intensity = 1 x 10^7/spill/each beam polarization with 1 spill/50 sec, and polarization P_B = 0.45

Geometrical Efficiency for π° detection = 0.25

Liquid H_2 target 100-cm long for A_N measurements

Polarized NH_3 target 10-cm long for A_{LL} measurements

The invariant cross section was calculated with the parametrization of Busser et al.

$$f = E\frac{d^3\sigma}{d^3p} = C\, p_\perp^{-n}\, e^{-bx_\perp},$$

where C = 14.2 x 10^{-27} cm^2/GeV^2, n = 8.6, and b = 12.5. The results are given in Table 2 for an integrated beam intensity of 3.6 x 10^{11} polarized protons corresponding to 600 hours running time.

The statistical error in A_N is

$$\Delta A_N \simeq \frac{\sqrt{\chi}}{P_B}\,\frac{1}{\sqrt{N_{Tot}}},$$

where $\chi = 1 + \frac{B}{S}$ and B/S = background over signal ratio.

In this case the backgrounds result largely from pairs of uncorrelated γ's which fall within the π^0-acceptance criteria. This background can be estimated from the 2γ effective-mass distributions. With $\chi = 1.1$ as a reasonable estimate we obtain the errors ΔA_N given in Table I.

SYSTEMATIC ERRORS:

The systematic errors divide roughly into multiplicative and additive. Uncertainties in target and beam polarizations are multiplicative errors. Target polarization can be measured to $\pm$ 3% with the principal uncertainty in calibration of the nuclear magnetic resonance system which uses the thermal equilibrium signal. It is estimated that beam polarization can be calculated to $\pm$ 3% from the beam optics. Nevertheless, we propose to measure this independently with a high-rate polarimeter based on elastic scattering in the Coulomb-nuclear interference region; this will provide an accuracy of $\pm$ 5% even for runs as short as a few hours.

Additive errors which may introduce a spurious asymmetry in the data can arise from

i) changes in beam geometry with reversal of beam polarization

ii) misalignment of detector components

iii) changes in gain of spectrometer elements.

Geometric sources of error associated with either the beam or detector can be accurately controlled through frequent cross-checks of counting rates with different spin-spin and spin-detector (right or left) combinations. The gain stability of the Pb-glass counters will be controlled to an accuracy better than 1%. With frequent reversals of beam polarization long-term variations in gain will average away.

This discussion on systematic errors also applies in part to C and D.

Table I

Estimates of Total Number of Events and Corresponding Error In A_N ($pp \to \pi^\circ x$) for 600-Hour Use of the Beam Time

$p_\perp$ (GeV/c)	$x_\perp$	Δx_F	$\Delta p_\perp$	n	ΔA_N %
2	0.21	0.1	0.5	3.2×10^6	$< \pm 0.12$
2.5	0.26	0.1	0.5	2.5×10^5	$< \pm 0.41$
3	0.31	0.125	1.0	6.7×10^4	$< \pm 0.8$
4	0.41	0.15	1.0	1.9×10^3	$< \pm 4.8$
5	0.52	0.20	1.0	9.9×10^1	$< \pm 21$

Estimates of Errors in A_{LL} ($pp \to \pi^\circ x$) Assuming 300-Hour Use of the Beam Time

$p_\perp$ (GeV/c)	ΔA_{LL}%
2.0	$< \pm 0.8$
2.5	$< \pm 3.0$
3.0	$< \pm 6.0$

C. High-x Charged Meson Production

The layout of the experimental apparatus is shown in Fig. 1.

The transversely polarized-proton beam is incident upon the 100-cm long liquid hydrogen target. To obtain adequate resolution in $p_\perp$, the angle of each incoming particle is measured by the two x-y hodoscopes HB_1 and HB_2.

The production angles of charged particles emerging from the target are measured in the multiwire proportional chambers (MWPC) PC1-PC5. Their angles, after bending in the BM109 for momentum analysis, are again measured in MWPC's PC6-PC9.

For π^- production, particle identification is simple due to the opposite curvature of pions and protons in the field of the BM109. We plan to trigger only on π^- produced to beam left; thus, at PC16 π^- are separated from the beam by .2 - .5 m. Simply placing a scintillation counter (labeled S_{π^-}) as shown should provide a clean trigger for π^-. The π^- trigger will be tightened further by requiring the threshold Cerenkov counter C2 in coincidence. We expect to be able to make reliable estimates of π^- asymmetries on line.

For π^+ production, particle identification is more difficult, especially at very high values of x. We plan to use the Cerenkov counters in coincidence to suppress background from proton induced δ-rays from the beam and the copious inelastically scattered protons ($p/\pi^+ = 10^3$ at $x = .9$). Each counter should discriminate against protons at a level $< 10^{-3}$; with the BM109 to sweep out delta rays produced upstream, we should get a total suppression of $\sim 10^{-5}$ of spurious proton triggers. We expect singles rates $\sim 10^5$/sec for each counter, but multiple-coincidence trigger requirements should eliminate this problem. The C_3 threshold setting along with the bend of the BM109 should strongly suppress triggers due to lower x pions ($p_{lab} \lesssim 50$ GeV/c). We plan to trigger the π^+ experiment by requiring a deflection in the downstream hodoscopes of at least 0.2 mrad corresponding to a cutoff $p_\perp \gtrsim .1$ GeV/c. There should be $\lesssim 10^4$ trigger candidates/burst, so that a clean decision can be made by the matrix coincidence electronics with little dead time.

RATES, RESOLUTION, AND RUN PLAN:

These are shown in Table II.

Table II

A Summary of the Expected Rates and Run Time

Reaction	Simultaneously Recorded Range $p_\perp$	x	I_o(ppp)/ Each Beam Polarization	ΔA	Beam time (hours) 60 pulses/hour
				10 bins of $p_\perp$ for $\Delta x = .05$	
$p\uparrow p \to \pi^+ x$	.1→1.0	.5→.85	10^7	$.01/p_B$	120
$p\uparrow p \to \pi^- x$	.1→1.0	.5→.9	10^7	$.015/p_B$	300
				5 bins of $p_\perp$ for $\Delta x = 0.5$	simultaneously recorded
$p\uparrow p \to \pi^+ x$	1.0→1.5	.5→.85	10^7	$.01/p_B$	600
$p\uparrow p \to \pi^- x$	1.0→1.5	.5→.9	10^7	$.02/p_B$	600
				TOTAL REQUEST	600 hours

The parametrizations of the inclusive scattering data by Johnson et al.[9] have been used for these rate estimates.

With the expected intensity and beam polarization ($I_o = 10^7$/pulse/each beam polarization and $P_B = .45$) we should be able to measure asymmetries covering the kinematic range $x = .5 \to .9$ and $p_\perp = 0.1 \to 1.5$ to an accuracy of at least .03 - .05 in the indicated 600 hours.

We expect to use a BM109 shimmed to a 6" gap as a spectrometer magnet, giving a 1.2-GeV/c transverse deflection. The angular resolution of the upstream hodoscopes H1 and H2 determine the resolution $\Delta p_\perp \tilde{=} .04$ GeV/c, and the MWPC's give $\Delta x \tilde{=} \pm .03$. Our resolution should enable measurement of the asymmetries in sufficiently small bins to determine the x and $p_\perp$ dependence.

If no sharp structure is observed binning can be broadened to reduce statistical errors.

We plan to explore quickly the high x, low-$p_\perp$ region during the beam tune-up period for possible large single-spin asymmetries for pions. If these are found, the apparatus could then be used as a relative polarimeter for further beam tune-up. If substantial asymmetries ($\sim .2 - .3$) are found, a polarimeter which measures $\Delta P_B/P_B = .05$ in $\sim$ 20 minutes can be effected with the same spectrometer.[10]

D. Large-x Λ°, K° Production

We concentrate here on the region of forward production with $0.5 \leq x \leq 0.8$ and $0.2 \leq p_\perp \leq 1.5$ GeV/c. Restriction to this kinematical region simplifies the apparatus with respect to the setup in P-677 and improves the compatibility with other measurements, while retaining the most accessible subject of current interest. Lambda particles are identified by detecting the $\Lambda^\circ \to p\pi^-$ decay in the magnetic spectrometer. Their polarization is measured by studying the angular distribution of the decay protons and pions.

In this way it should be possible to obtain simultaneously a measurement of the production asymmetry A_N, the final lambda particle polarization P_o (averaged with beam polarization), and the depolarization tensor component D_{NN} representing the fraction of the initial beam polarization attained by the final Λ°. Simultaneously with the $pp \to \Lambda^\circ X$ measurement also data on K° production would be obtained, providing a measurement of the production asymmetry A_N for $pp \to K^\circ X$.

The relative distribution of momentum in the $\pi^+\pi^-$ pair from the K° decay is distinctively different from that of the $p\pi^-$ pair from Λ°: the discrimination between K_o and Λ° will be improved by using the information from Cerenkov counters C2 and C3 together with momentum measurements.

The high energy Λ° of interest in the considered kinematic region will have in the characteristic Y-shaped pattern of decay, as both the particles in the pair are originally produced with a small relative angle with respect to the neutral parent and are opened up by the analyzing magnetic field.

To simplify the selection schemes, we accept only Λ° produced to the right of the beam; in this case the decay protons are all bent by the magnetic field to the right of the deflected non-interacting beam; the pions are bent the opposite way and end-up in separate regions of PC9 and H4.

Triggering schemes involve the following conditions:

— A beam particle defined with hodoscopes HB,1,2

— A veto for non-interacting beam with HB4,5,6

— A "neutral decay" flag in the region of DR (a vacuum decay volume, to minimize charged and neutral particles' interactions that might fake a decay) obtained by multiplicity comparison in HB3,H1 and in solid-state detectors MSD1,2.

— A correlation in space and time between decay proton and pions in the hodoscope H2, H3 and H4.

The direction and the momenta of the produced particles are determined by proportional chambers PC2-PC11 before and after the magnet. Information from the chambers is fed to on line processors to correlate the tracks in the spectrometer and check for the characteristic "Y-shaped" pattern of Λ°

decay. We expect that these selection criteria would greatly reduce the background from directly produced charged particles and combinatorial background.

Estimates of Rates and Asymmetry Precision

Using an experimental parametrization (19) of the differential cross-section for the reaction $pp \to \Lambda^\circ X$, the number of events produced in each $(x, p_\perp^2)$ bin is estimated for a beam of 10^7 polarized protons per spill with 60-second repetition period, impinging on a 100-cm long liquid hydrogen target.

For 600 hours of running time the statistical accuracy ΔA_N achieved in the asymmetry measurement is shown in Fig. 4 as a function of x and $p_\perp^2$, assuming a 45% beam polarization and a 1:2 background-to-signal ratio. Typical values for ΔA_N and ΔD_{NN} at $0.5 \leq x \leq 0.8$ are:

Table III

Statistical Errors in Λ° Experiment in % for 610-Hour Use of the Beam Time

	$p_\perp^2 =$	$0.3 \pm .06$	$0.8 \pm .24$	1.8 ± 0.7 $(GeV/c)^2$
ΔA_N	Λ°	$\approx 0.2\%$	0.5	4.0
	K°	0.5	3.0	15.
ΔD_{NN}	Λ°	0.8	2.0	15.

(Note: 10^7 protons/spill/each beam polarization would yield smaller statistical error than those quoted above.)

Systematic errors which might produce spurious asymmetries are suppressed by frequent flipping of the beam polarization and by changing the polarity of the spectrometer magnets and measuring the left-right asymmetries.

V. Equipment Needed

Equipment Needed	Expt.: $\Delta\sigma_L$	$\pi^{\pm}$ Large x	Λ° Large x	π° Large $p_{\perp}$	Requested from Fermilab
Beam Hodoscopes	X	X	X	X	
Snake	X	X	X	X	
Beam Cerenkov	X				
Beam Polarimeter	X	X	X	X	
Polarized Target	X				
Liquid Hydrogen Target		X	X	X	X
Anal. Magnet BM109	X	X	X		If Super-conducting
Transmission Hodoscope	X				
Trigger Hodoscopes		X	X	X	
Cerenkov Counters	X	X	X		
Lead-glass Counters				X	
Proportional Chambers		X	X	X	
Multi-strip Sol. State Detector			X		
NIM Electronics	X	X	X	X	Partial
Wire Chamber Read-Out		X	X	X	
Fast ADC				X	
Camac Electronics	X	X	X	X	Partial
On-line Processor			X	X	
On-line Computer	X	X	X	X	Partial

References

1. R. D. Klem et al., Phys. Rev. Lett. 36, 929 (1976); W. H. Dragoset, Jr. et al., Phys. Rev. D18, 3939 (1978).

2 J. Antille et al., Phys. Lett. 94B, 523 (1980).

3. D. G. Crabb et al., Phys. Rev. Lett. 41, 1257 (1978).

4. K. Heller et al., Phys. Rev. Lett. 41, 607 (1978).

5. M. J. Alguard et al., Phys. Rev. Lett. 37, 1258 (1976); Phys. Rev. Lett. 37, 1261 (1976); Phys. Rev. Lett. 41, 70 (1978); Madison Conference, 1980.

6. See for instance, A. Yokosawa, Phys. Reports 64, 47 (1980).

7. K. Kuroda et al., "A Scintillation Target for the Calibration of High Energy Polarized Beams", paper presented at the 1980 International Symposium on High Energy Physics with Polarized Beams and Polarized Targets, Lausanne, Switzerland September 1980.

8. I. P. Auer et al., Phys. Rev. Lett. 41, 354 (1978).

9. J. R. Johnson et al., Phys. Rev. Lett. 39, 1173 (1977), and Phys. Rev. D17, 1292 (1978).

10. J. B. Roberts, Higher Energy Polarized Proton Beams, AIP Conf. Proc. No. 42, A. D. Krisch and A. J. Salthouse, editors, p. 67.

Figure Captions

Figure 1

HB 1,2	Beam Hodoscope
HB 3...6	Transmission Hodoscopes
Target	Target PPT or LH_2
H1...4	Trigger Hodoscopes
C1...3	Cerenkov Counters
G 1,2	Lead Glass Photon Calorimeters
V1, V2	Veto Hodoscopes
MSD1,2	Multistep Solid-State Detectors
DR	Λ° Decay Region
PC1-9	MWPC for $\pi^\pm$ and $\Lambda^\circ \to p\pi^-$
PC10-15	MWPC for tracking charged particles in lead glass and for vertex finding
PC16	MWPC to increase resolution for $\pi^\pm$

Figure 2 Acceptance of gamma detector.

Figure 3 Two-gamma spectrometer.

Figure 4 Statistical accuracy vs. x and $p_\perp^2$.

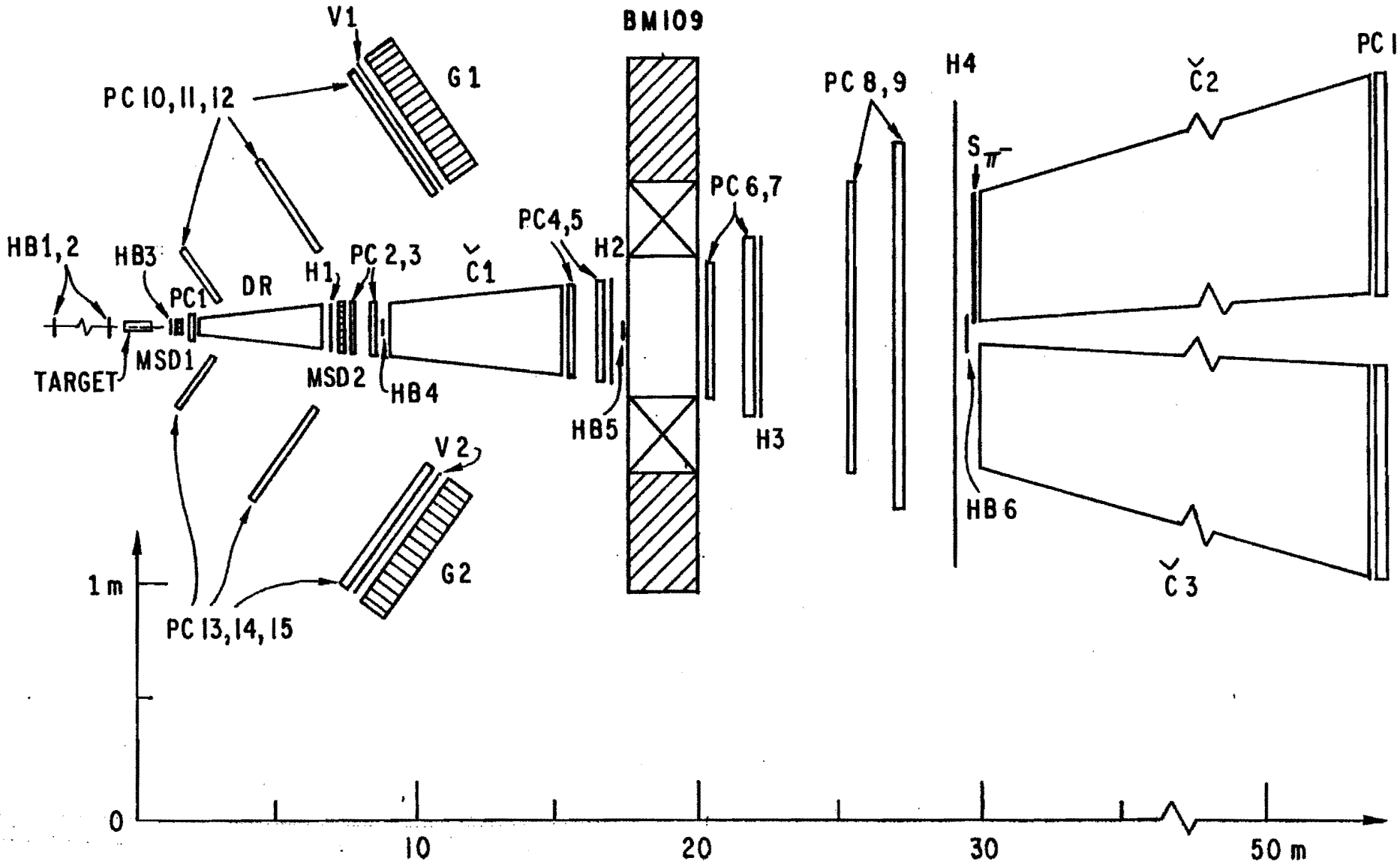
V1
BM109
G1
PC 10,11,12
PC 16
PC 8,9
H4
C2
S π⁻
PC 6,7
PC4,5
H2
HB1,2
HB3
PC 2,3
C1
H1
PC1
DR
TARGET
MSD1
MSD2
HB4
HB5
H3
V2
HB 6
C3
G2
1 m
PC 13,14,15
0
10
20
30
50 m

Figure 1

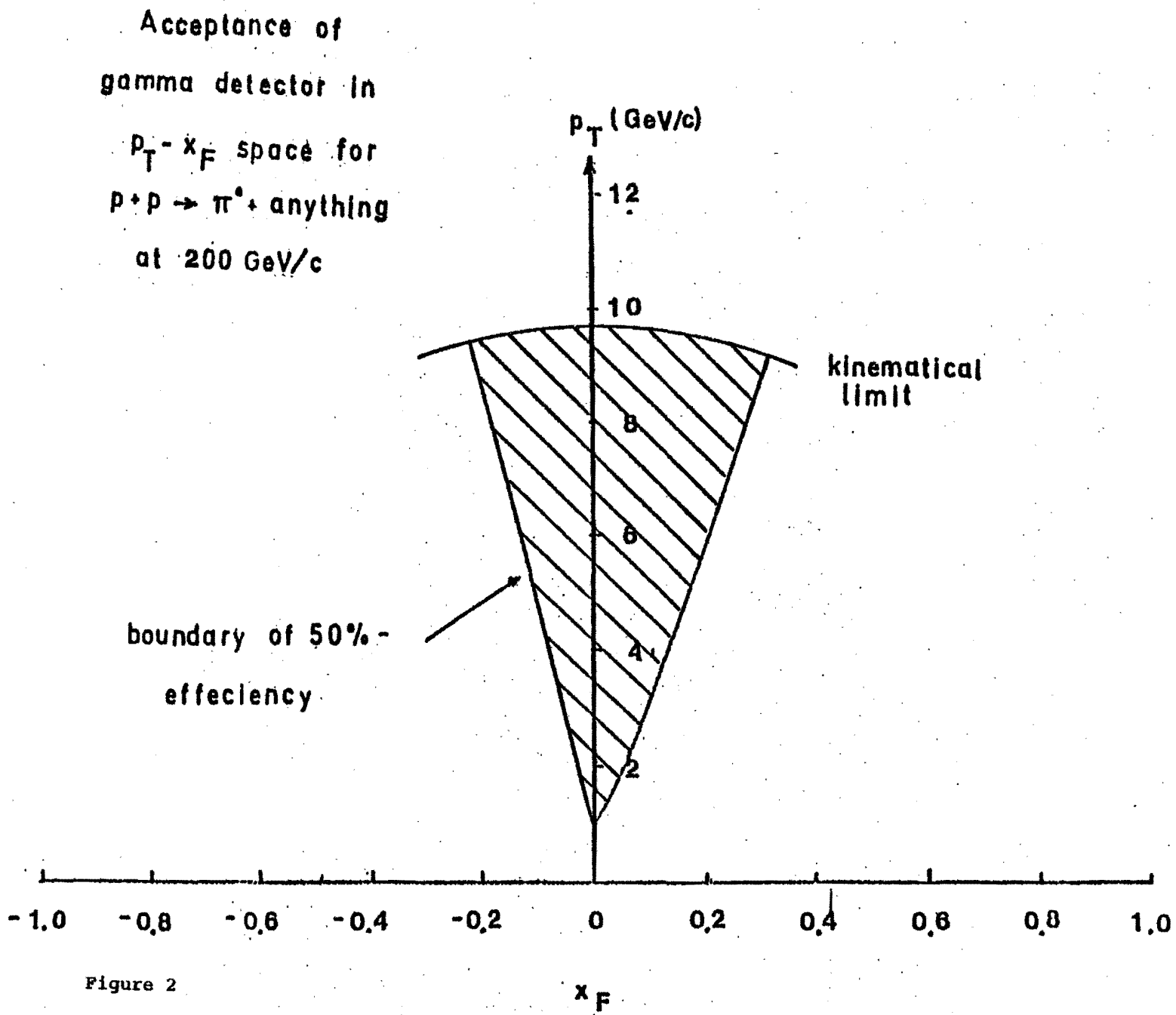
Acceptance of
gamma detector in
$p_T - x_F$ space for
$p + p \rightarrow \pi^0 +$ anything
at 200 GeV/c
p_T (GeV/c)
12
10
8
6
4
2
kinematical
limit
boundary of 50% -
effeciency
-1.0
-0.8
-0.6
-0.4
-0.2
0
0.2
0.4
0.6
0.8
1.0
x_F

Figure 2

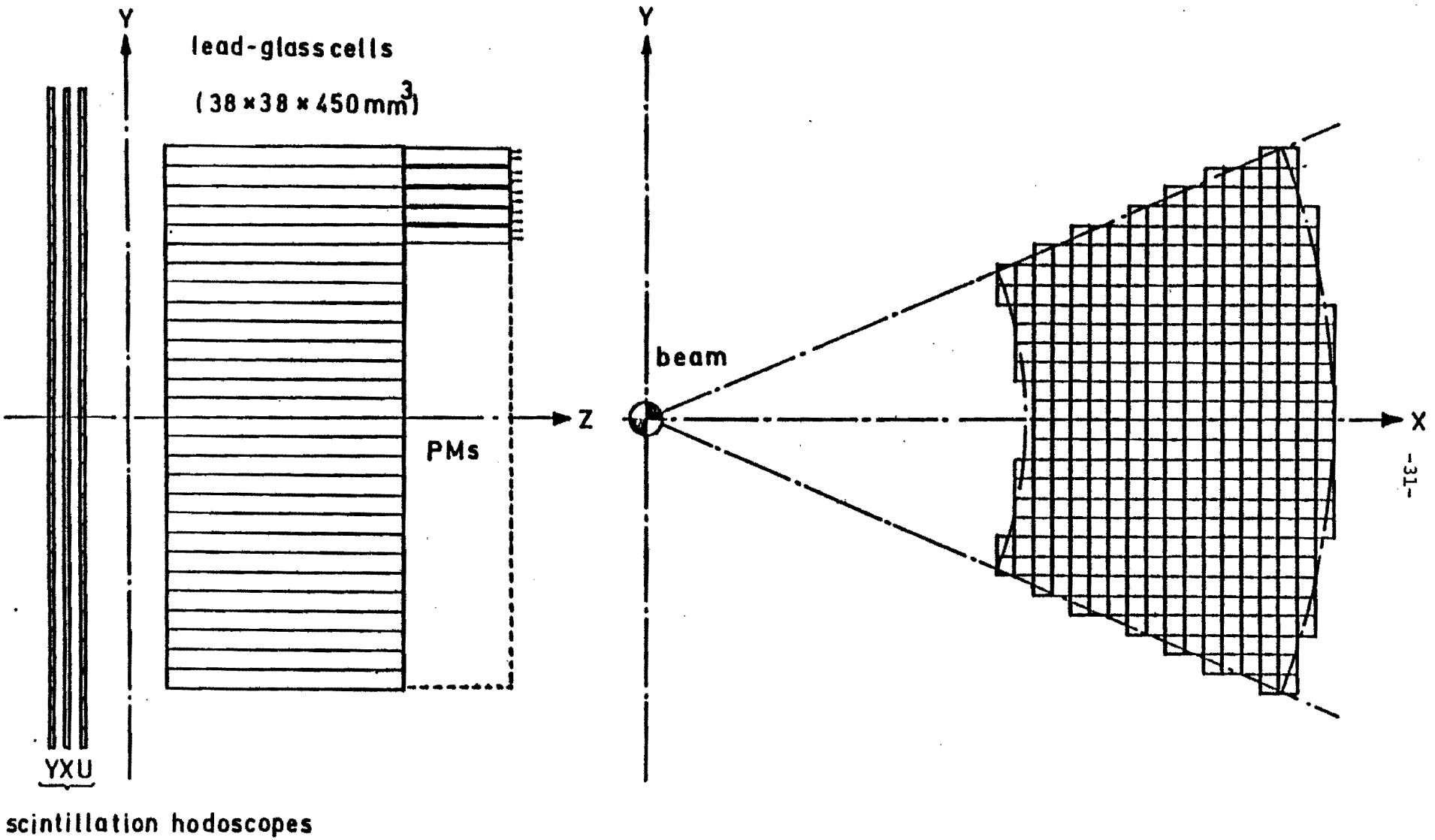
Y
lead-glass cells
(38 × 38 × 450 mm³)
Z
PMs
YXU
scintillation hodoscopes
Y
beam
X

Figure 3

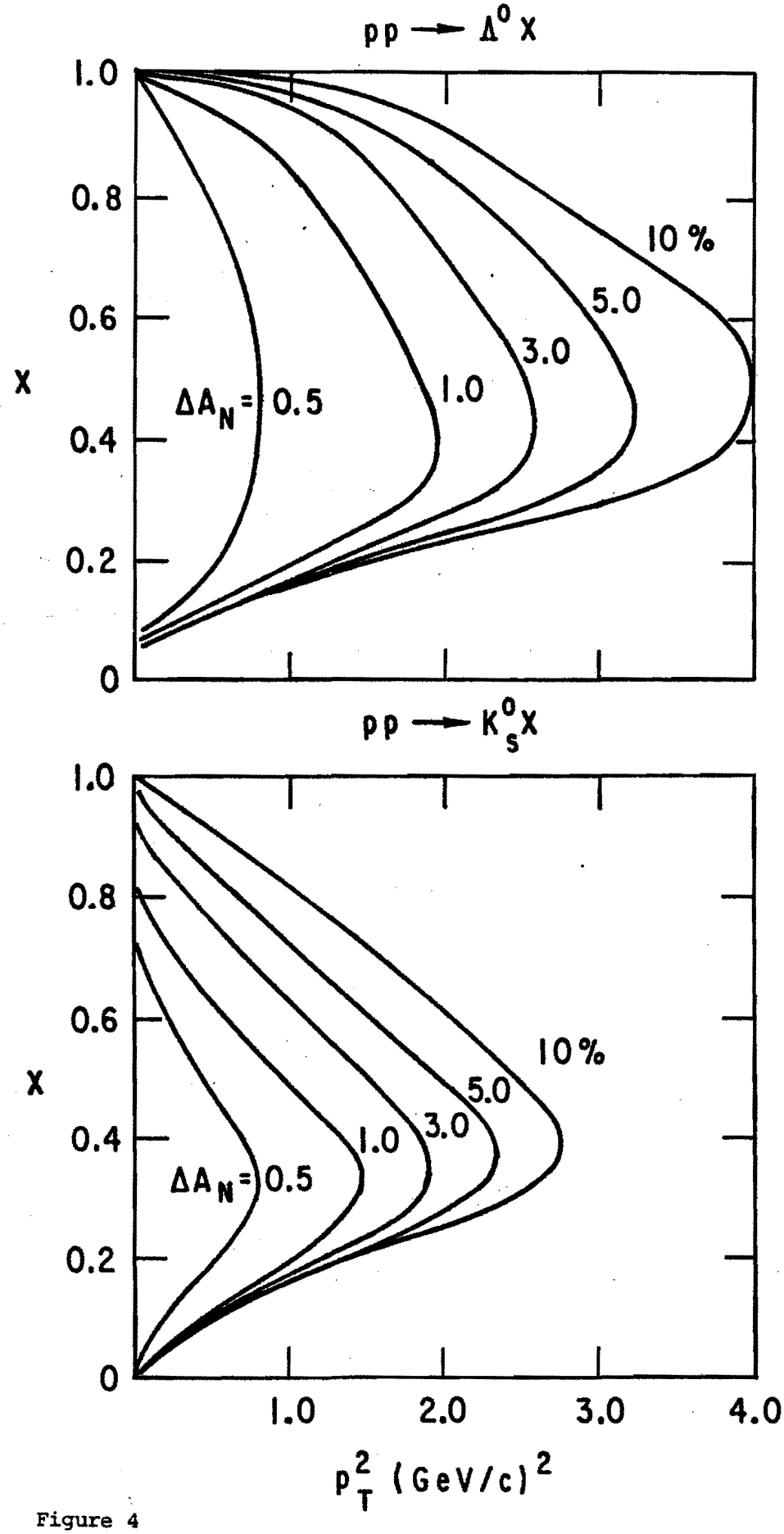
pp → Λ⁰X
1.0
0.8
0.6
0.4
0.2
0
X
ΔA_N = 0.5
1.0
3.0
5.0
10 %
pp → K⁰_S X
1.0
0.8
0.6
0.4
0.2
0
X
ΔA_N = 0.5
1.0
3.0
5.0
10 %
1.0
2.0
3.0
4.0
p²_T (GeV/c)²

Figure 4

ADDENDUM to E-704

21 September 1990

A_{LL} Measurements in $\chi 2$ Production Simultaneously Performed With π° Production at 200 GeV/c

Abstract

For the next fixed-target period, we have requested to complete $A_{LL}(pp)$ measurements in π° production at 200 GeV/c. We would like to simultaneously measure the parameter A_{LL} in $\chi 2$ production utilizing the CEMC (central electromagnetic calorimeter). We expect to have a good chance of determining the spin-dependent gluon structure function around an x range centered at 0.175, since the $\chi 2$ production is dominated by gluon-gluon fusion.

I. Introduction

To understand the basic question of the origin of proton spin, we propose to study the gluon spin distribution in the proton by measuring the spin correlation parameter A_{LL} in the $\chi 2$ production, with longitudinally polarized protons on longitudinally polarized target nucleons.

The major detector for the $\chi 2$ measurements will be the CEMC consisting of 2,000 lead-glass counters and an electromagnetic calorimeter consisting of CsI blocks. We will introduce a new trigger scheme to enable the simultaneous measurements of π° and $\chi 2$.

II) Physics Goals ($\chi 2$ production and two-spin asymmetry, A_{LL})

Results of recent experiments to determine the spin-dependent structure function of the proton by the EMC group[1] have been interpreted to mean that the proton spin may not be due to the helicity of its constituent quarks.

Instead, most of the proton spin may be due to gluons and/or orbital angular momentum.[2]

The double-spin asymmetry, A_{LL}, in $p^{\uparrow}p^{\uparrow} \rightarrow \chi 2\ (3555) \rightarrow J/\psi + \gamma$ is expected to provide a means to study the spin-dependent gluon structure function. The 15% decay branching ratio of $\chi 2\ (3555)$ to $(J/\psi + \gamma)$ allows us to analyze the helicity of the charmonium state.

There is general agreement[3] theoretically that $\chi 2\ (3555)$ state is mainly produced by gluon-gluon fusion as shown below and there are promising experimental results[4] suggesting that simple gluon fusion is sufficient to account for the $\chi 2\ (3555)$ production in proton interactions at 200 and 250 GeV/c.

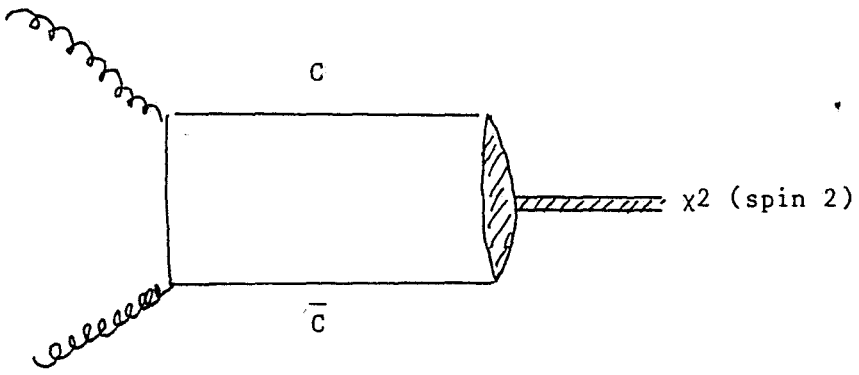

The measured two-spin asymmetries (as defined below) give information on the initial gluon polarization, which can be used to reconstruct the gluon spin distribution in the polarized proton.[5]

$$A_{LL} = (1/P_B P_T^{eff}) \frac{N\left(\overset{\rightarrow}{\rightarrow}\right) - N\left(\overset{\leftarrow}{\rightarrow}\right)}{N\left(\overset{\rightarrow}{\rightarrow}\right) + N\left(\overset{\leftarrow}{\rightarrow}\right)}, \qquad (1)$$

where P_B is beam polarization, P_T^{eff} is effective target polarization, and arrows indicate the spin direction in the laboratory system. By considering the above diagram, if the initial helicity state is (+-), that is $\left(\overset{\uparrow}{\downarrow}\right)$, then $J_z = 2$ and this state produces $\chi 2$.

To be exact, the observable A_{LL} is related to the distribution function of a polarized gluon in a polarized proton expressed as $G_+(x)$ and $G_-(x)$ with same- and opposite-sign helicities respectively.[5]

$$A_{LL}\ (x_F) = (1-R)/(1+R)\ \left[\frac{\Delta G}{G}\ (x_1) \cdot \frac{\Delta G}{G}\ (x_2)\right]; \qquad (2)$$

where x_1, x_2, and x_F are the longitudinal-momentum fraction of gluons, R is the ratio of matrix elements f_+ (f_-) which are the squared matrix elements for the production of $\chi 2$ out of two gluons with same- (opposite-) sign helicities, and $\Delta G/G\ (x) \equiv (G_+(x) - G_-(x))/(G_+(x) + G_-(x))$. The $R = f_-/f_+$ can be determined experimentally as shown in Appendix I and also can be theoretically estimated.

III) Experimental Setup

Schematic view of the experimental arrangement is shown in Figs. 1 and 2, which consist of

- Electromagnetic calorimeters
- Proportional chambers
- Plastic scintillator pad for charged trigger

Electromagnetic Calorimeters

In order to separate χ_1 (3510 MeV) and χ_2 (3555 MeV) peaks, the energy resolution of the calorimeter is important, especially for the produced γ's. According to the decay kinematics of χ_2, the γ's are effectively detected in the very forward angle (< 80 mrad). A calorimeter for detection of these γ's must have fast response with high energy resolution.

The central part (12 mrad < θ_{lab} < 60 mrad) of the calorimeter system consists of pure CsI blocks (3.8 x 3.8 x 40 cm^3) to ensure good energy resolution of the γ detection. Pure CsI has two components (310 nm and 480-600 nm) of scintillation pulse. The fast component (310 nm) has decay time of 20 nsec while the slow component has a decay time of 3 μsec.[6] By filtering the slower component optically, pure CsI becomes high-resolution fast-response calorimeter. The energy resolution of 2% at E = 1 GeV has been measured.[6] The characteristics of pure CsI are compared with other scintillators in Appendix II.

The CEMC covers a large area (60 mrad < θ_{lab} < 130 mrad). The CEMC + CsI calorimeters cover x_F = -0.3 to 0.6. These lead glass blocks have been used in the earlier E-704 experiment for high-$p_\perp$ π° detection as demonstrated in Fig. 3. The corresponding energy resolution is $(2 + 5/\sqrt{E})$%.

We note that the $\chi 2$ states have been detected[7] by measuring e^+, e^-, and γ utilizing a calorimeter similar to the CEMC. In the proposed experiment $\chi 1$ and $\chi 2$ must be separated. We have made Monte Carlo calculations assuming the 2-mm position resolution and $(1\% + 1\%/\sqrt{E})$ energy resolution on the CsI detector in order to estimate the overall mass resolution of $\chi 2 \rightarrow J/\psi + \gamma \rightarrow e^+e^-\gamma$. The results are shown in Fig. 4.

The proportional chambers placed between the target and the CEMC serve to track e^+ and e^- particles and assure that there are no charged tracks in the γ direction.

Scintillator Pad

The scintillator pad detector has a segmented mosaic structure as shown in Fig. 5. Size of the segmentation is determined to minimize chance coincidence of γ with charged particles.

Trigger Scheme

The basic idea of the J/ψ trigger is to obtain $p_\perp$ signals and their summation from the calorimeter only for electrons. To achieve this we introduce a super-block which consists of several calorimeter blocks. The size of a super-block is defined by the scintillator pad. All the calorimeter blocks, under one super-block, are summed providing $p_\perp$ (super-block) signal.

The $p_\perp$ (super-block) signal is to be discriminated at 0.6 GeV in $p_\perp$ to eliminate many of the charged pions. This discriminated signal in coincidence with a corresponding hit in the scintillator pad provides electron candidates. This coincidence will eliminate γ's.

The electron candidate signal opens an analogue switch to make a $p_\perp$ summation only for the electron candidate. This summed signal is called $\Sigma p_\perp$ (super-block).

J/ψ trigger candidate requires:

- 2 or more electron candidates and
- $\Sigma p_\perp$ (super-block) to be greater than 2.5 GeV.

The $\Sigma p_\perp$ (super-block) signal roughly corresponds to the J/ψ mass. See Monte Carlo results of the $p_\perp$ correlation of the two decay electrons (Fig. 6).

According to the trigger rate study by using LUND and GEANT, described in detail in the next chapter, 2×10^7 200-GeV beam on the LiD target will give 43 fake J/ψ triggers/spill with this scheme due to the hadronic background. We can handle this trigger rate with an existing data acquisition system.

Beam and Target

This measurement will be simultaneously carried out with the A_{LL} (π°) run and there is no special beam and target requirement (beam time: 8-months x 40%).

IV) Event Rate and Background Consideration

We discuss the event rate of J/ψ and χ_2 in the trigger scheme described in the previous section. We also estimate the background and the mass spectra.

Event Rate

To estimate the good event rate we made Monte Carlo calculations with the following conditions:

- The χ_2 production cross section was assumed to be 50% of the J/ψ production cross section.[4] The $p_\perp$ and x_F distributions of χ_2 were assumed to be the same as those of J/ψ.
- The J/ψ production cross section at 200 GeV is taken to be 20nb.[8]
- The isotropic decay of $\chi 2 \rightarrow J/\psi + \gamma$ is assumed. (This condition depends on the mixture of different J_z states. See previous section for details.)
- Losses due to the target material (20-cm long, 3-cm diameter LiD) are included.
- Intensity/spill = 2×10^7 polarized-protons/spill on 20-cm LiD target.
- 183 cm x 183 cm lead-glass calorimeter at z = 6.5 m from the target with 76.4 cm x 76.4 cm CsI around the center and a 15.3 cm x 15.3 cm hole. γ's from $\chi 2$ are required to hit the CsI part.

As the results for the geometrical acceptance, we obtain 25,000 events/(800-hour beam) of $J/\psi \rightarrow e^+e^-$ and 5,000 events/(800-hour beam) of $\chi_2 \rightarrow J/\psi + \gamma$, which correspond to 0.6 and 0.12/spill respectively.

Background Estimation

As the source of the background we can list:

- π's interacted in the calorimeter

- γ overlapped with charged particles in a super-block
- γ from hadronic decays converted to e^+e^-

To estimate these backgrounds, we generated proton-proton hard-collision events in our experimental configuration. LUND (PYTHIA) and GEANT were used for this Monte Carlo. For energy deposition by hadrons in the calorimeter, the results of measurements by S. Orito et al.[9] were used. The secondary interactions in the target were included in the calculation.

We apply the trigger condition as described in the previous section. We required:

- More than 2 electron candidates which have $p_\perp$ (super-block) of 0.6 GeV
- $\Sigma p_\perp$ (super-block) being greater than 2.5 GeV

The calculated trigger rate is 43/spill while these kinematic thresholds pass 80% of J/ψ events. 35% of this trigger is by electrons from converted γ's, and the rest is by charged hadrons overlapped with γ's.

After the trigger simulation we apply offline cut to check the background in the e^+e^- spectrum.

1. $p_{\perp 1} > 0.6$ GeV, $p_{\perp 2} > 0.6$ GeV, and $p_{\perp 1} + p_{\perp 2} > 2.5$ GeV,
2. Invariant mass of the charged pair is between 2.8 to 3.2 GeV
3. Transverse shower spread cut[a]

The background rate to the J/ψ signal is found to be 33% in the J/ψ mass range. The background rate to the $\chi 2$ is about 10%, which is combinatorial background of J/ψ + γ (γ from light meson decay).

---

[a] The hadron rejection by cutting on transverse shower spread is a factor of 10 for each hadron, according to V. A. Davydov et al.[10]

V) Determination of $\Delta G/G$ (x)

In the gluon fusion process, the following relations are apparent:

$$x_1 - x_2 - x_F = 0,$$
$$x_1 x_2 - M^2/S = 0,$$

where M is the χ_2 mass and S is the beam energy in the center of mass. These relation connects the measured x_F distribution of χ_2 with the gluon structure function via Eq. (2). Our geometrical acceptance centers at $x_F = 0$ where $x_1 = x_2 = 0.175$.

After integrating the x_F acceptance, 2000h beam time will give $\Delta A_{LL} = \pm 0.02$ for J/ψ production and $\Delta A_{LL} = \pm 0.05$ for χ2 production.

We illustrate the scope of our measurements using a simple model[11] of $\frac{\Delta G}{G}(x)$, which gives $\frac{\Delta G}{G}(x) = 1$ in the region $x > x_c$ and $\frac{\Delta G}{G}(x) = x/x_c$ in the region $x_c < x$. Figure 7 shows calculated values of $[\Delta G/G\ (x_1) \cdot \Delta G/G\ (x_2)]$ vs. x_F of χ2.

When we assume $x_c = 0.2$ as preferred in Ref. 11, then $\Delta G/G(x) = 0.9$ at $x = 0.175$. By further assuming $R = 0.2$ in Eq. (2), we then obtain $A_{LL} = 0.6$. In this case, our measurement will yield $A_{LL} = 0.60 \pm 0.05$ or $(\Delta G/G)^2 = 0.80 \pm 0.07$.

REFERENCES

1) J. Ashman et al. Phys. Lett. B206, 364 (1988); Nucl. Phys. B238, 1 (1989).

2) For instance, see S. J. Brodsky, J. Ellis, and M. Karliner, Phys. Lett. B206, 309 (1988).

3) S. D. Ellis et al., Phys. Rev. Lett. 36, 1263 (1976); B. L. Ioffe, Phys. Rev. Lett. 39, 1589 (1977); C. E. Carlson et al., Phys. Rev. D18, 760 (1978); H. Fritzsch, Phys. Lett. 67B, 217 (1977); M. Gluck et al., Phys. Rev. D17, 2324 (1978); L. M. Jones et al., Phys. Rev. D17, 1782 (1978); V. Berger et al., Z Phys. C6, 169 (1980); J. H. Kuhn, Phys. Lett. 89B, 385 (1980); Y. Afek et al., Phys. Rev. D22, 86 (1980).

4) D. A. Bauer et al., Phys. Rev. Lett., 54, 753 (1985); Y. Lemoigne et al., Phys. Lett. 113B, 509 (1982).

5) J. L. Cortes and B. Pire, Phys. Rev. 38, 3586 (RC) (1988).

6) H. Kobayashi et al., Nucl. Instrum. and Meth., to appear.

7) F. Binon et al., Nucl. Phys. B239, 371 (1984).

8) J. G. Branson et al. Phys. Rev. Lett. 38, 1331 (1977), and references therein.

9) S. Orito et al., Nucl. Instr. and Meth. 215, 93 (1983).

10) V. A. Davydov et al., Nucl. Instr. and Meth. 145, 267 (1977).

11) E. L. Berger and J. W. Qiu, Phys. Rev. D40, 778 (1989).

APPENDIX I

Determination of $R = f_-/f_+$

The ratio of matrix elements f_-/f_+ can be determined from the angular distribution of the unpolarized case as[5]

$$\frac{1}{\sigma}\ \frac{d\sigma}{d\cos\theta} = \frac{1 - (1-R)\ 3/8\ (1 + \cos^2\theta)}{1 + R},$$

where θ is the angles between the photon and beam momenta in the $\chi 2$ rest frame.

APPENDIX II

Comparison of Scintillating Materials

Characteristics of pure CsI with other non-organic scintillator is shown in the table.

	Density	Ref. Index	Radiation Length (cm)	Decay Const. (ns)	Wave-Length (nm)	Light Yield Photons/MeV
CsI (pure)	4.51	1.80	1.86	fast:20/5 slow:3μsec	310 480-600	2000
BaF2	4.88	1.49	2.03	620/0.6	225/310	6500
BGO	7.13	2.15	1.12	300/60	480	8200
NaI(Tl)	3.67	1.85	2.59	230	410	38000

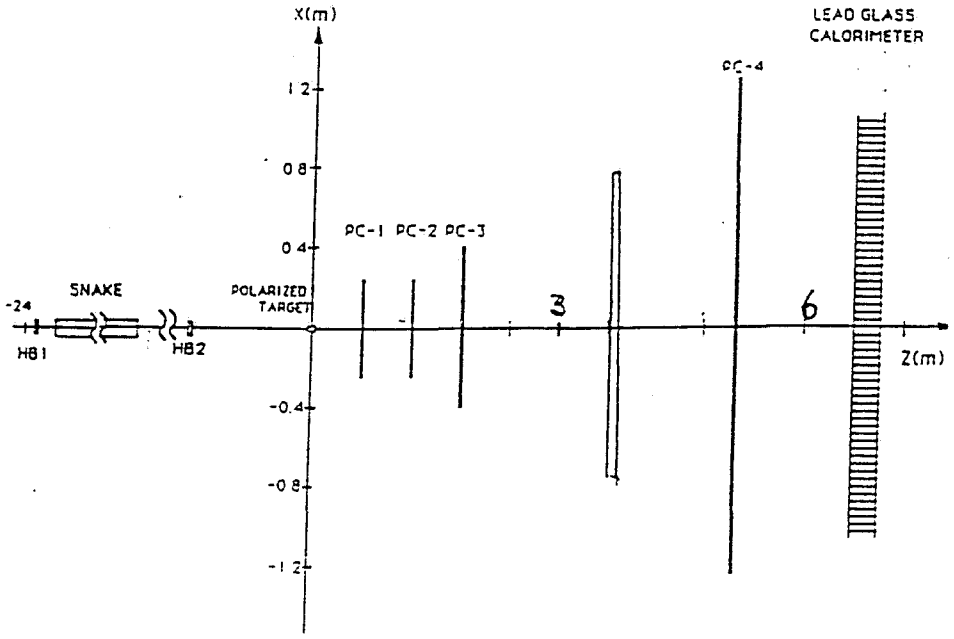

Figure 1

The schematic view of the experimental arrangement.

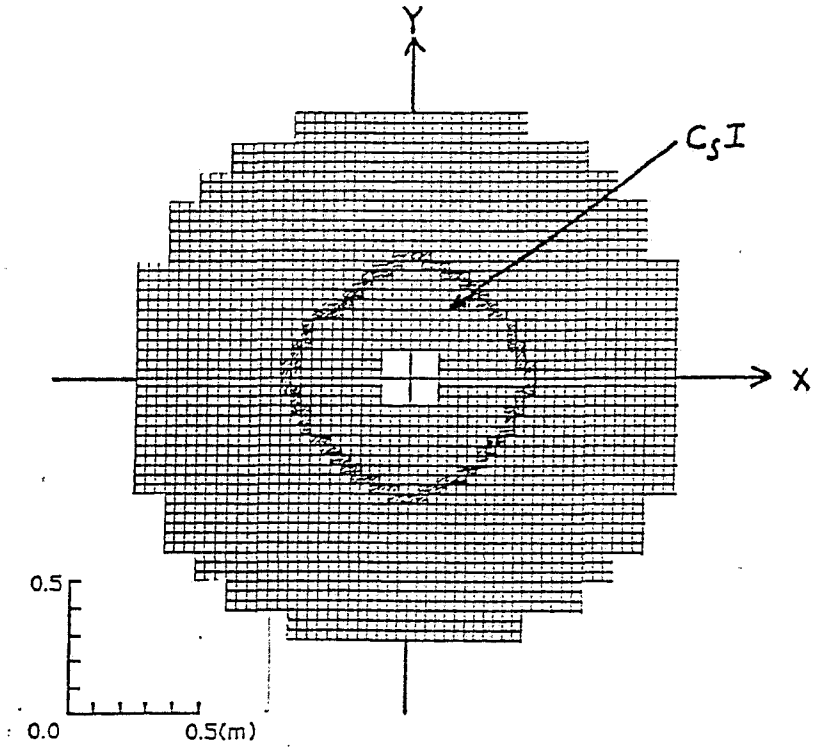

Figure 2

The front view of the EM calorimeter. The central part consists of pure CsI blocks and lead glass blocks (3.8 x 3.8 x 45 cm^3).

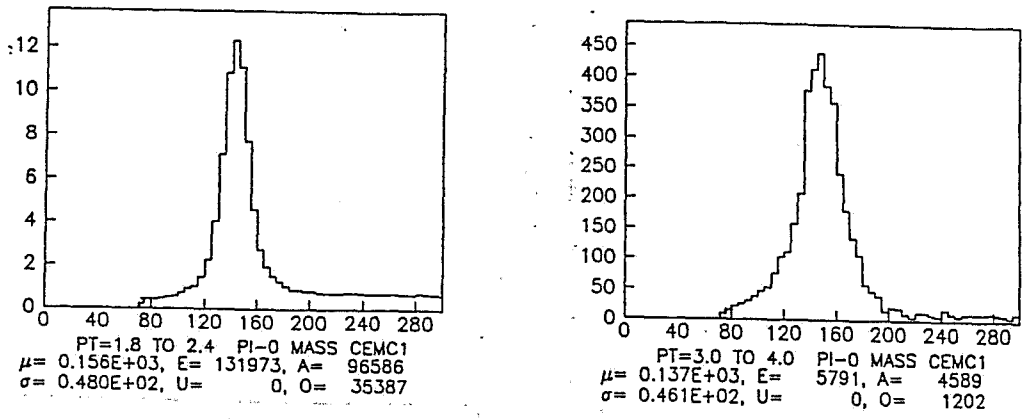

Figure 3 Mass distribution of π° measured by the existing lead glass calorimeter in E-704.

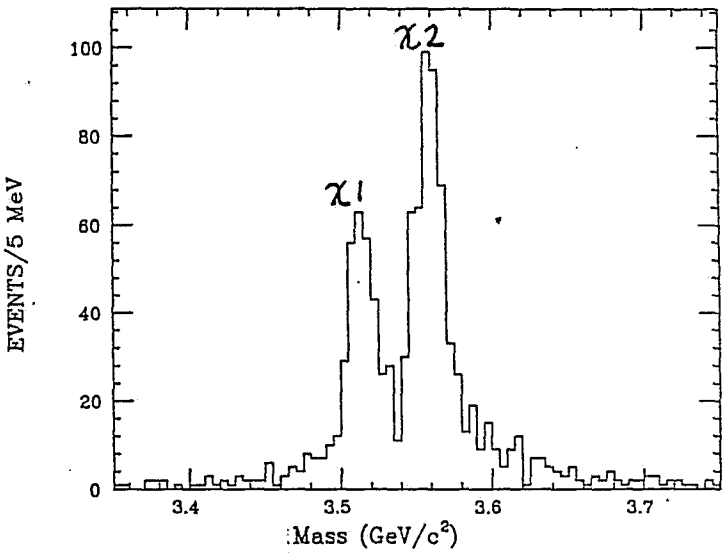

Figure 4 Generated mass distribution of $J/\psi + \gamma$ in the proposed setup. (J/ψ mass is fixed to 3100 MeV.)

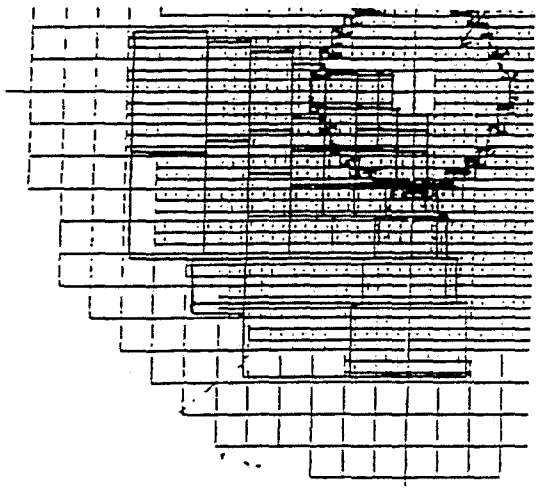

Figure 5 Schematic view of the scintillator pad detector having projective matching to the EM calorimeter. Each pad defines a super-block (see text).

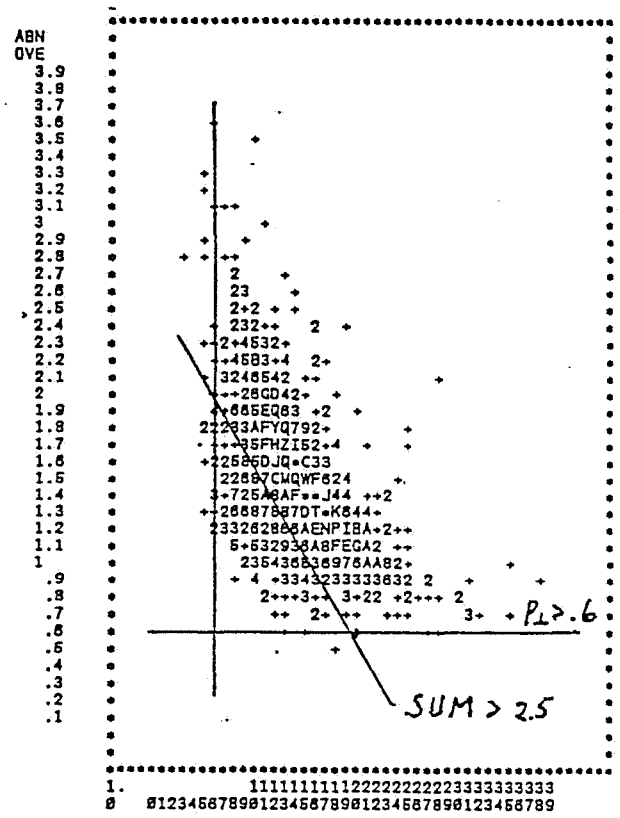

Figure 6

Generated $p_\perp$ correlation of electrons and positrons from J/ψ decay. See text for detailed description of the Monte Carlo calculation.

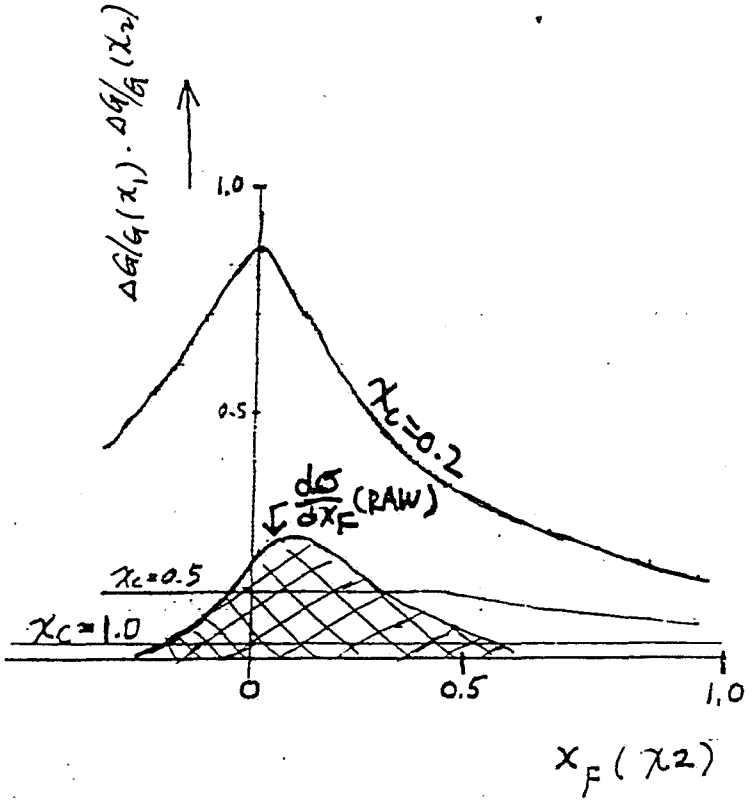

Figure 7

$\Delta G/G\ (x_1) \cdot \Delta G/G\ (x_2)$ vs x_F for x_c = 0.2, 0.5, and 1.0 (see text), and also expected x_F distribution for detected $\chi 2$.